Title
Nondestructive assessment of collagen hydrogel cross-linking using time-resolved autofluorescence imaging

Journal
Journal of Biomedical Optics, 23(3)

ISSN
1083-3668

Authors
Sherlock, Benjamin E
Harvestine, Jenna N
Mitra, Debika
et al.

Publication Date
2018-03-01

DOI
10.1117/1.jbo.23.3.036004

Peer reviewed

Journal of Biomedical Optics

BiomedicalOptics.SPIEDigitalLibrary.org

Nondestructive assessment of collagen hydrogel cross-linking using time-resolved autofluorescence imaging

Benjamin E. Sherlock
Jenna N. Harvestine
Debika Mitra
Anne Haudenschild
Jerry Hu
Kyriacos A. Athanasiou
J. Kent Leach
Laura Marcu

Benjamin E. Sherlock, Jenna N. Harvestine, Debika Mitra, Anne Haudenschild, Jerry Hu, Kyriacos A. Athanasiou, J. Kent Leach, Laura Marcu, "Nondestructive assessment of collagen hydrogel cross-linking using time-resolved autofluorescence imaging," *J. Biomed. Opt.* **23**(3), 036004 (2018), doi: 10.1117/1.JBO.23.3.036004.

Journal of Biomedical Optics 23(3), 036004 (March 2018)

Nondestructive assessment of collagen hydrogel cross-linking using time-resolved autofluorescence imaging

Benjamin E. Sherlock,[a,*] Jenna N. Harvestine,[a] Debika Mitra,[a] Anne Haudenschild,[a] Jerry Hu,[a] Kyriacos A. Athanasiou,[a,b] J. Kent Leach,[a,b] and Laura Marcu[a,*]
[a]University of California, Davis, Department of Biomedical Engineering, Davis, California, United States
[b]UC Davis Health, Department of Orthopaedic Surgery, Sacramento, California, United States

Abstract. We investigate the use of a fiber-based, multispectral fluorescence lifetime imaging (FLIm) system to nondestructively monitor changes in mechanical properties of collagen hydrogels caused by controlled application of widely used cross-linking agents, glutaraldehyde (GTA) and ribose. Postcross-linking, fluorescence lifetime images are acquired prior to the hydrogels being processed by rheological or tensile testing to directly probe gel mechanical properties. To preserve the sterility of the ribose-treated gels, FLIm is performed inside a biosafety cabinet (BSC). A pairwise correlation analysis is used to quantify the relationship between mean hydrogel fluorescence lifetimes and the storage or Young's moduli of the gels. In the GTA study, we observe strong and specific correlations between fluorescence lifetime and the storage and Young's moduli. Similar correlations are not observed in the ribose study and we postulate a reason for this. Finally, we demonstrate the ability of FLIm to longitudinally monitor dynamic cross-link formation. The strength of the GTA correlations and deployment of our fiber-based FLIm system inside the aseptic environment of a BSC suggests that this technique may be a valuable tool for the tissue engineering community where longitudinal assessment of tissue construct maturation *in vitro* is highly desirable. [DOI: 10.1117/1.JBO.23.3.036004]

Keywords: fluorescence lifetime; collagen; cross-link; nondestructive; hydrogel.

Paper 170372R received Jun. 7, 2017; accepted for publication Jan. 31, 2018; published online Mar. 6, 2018.

1 Introduction

The scarcity of quantitative, nondestructive assessment techniques for engineered tissues presents a critical bottleneck in the field of regenerative medicine. Conventional biochemical and mechanical tests are often time-consuming and damaging to structure and function of the sample under test, thereby reducing the available tissue for subsequent implantation. Nondestructive measurement techniques have the potential to lower costs and increase sample throughput, while providing an opportunity for a better understanding of sample maturation via repeated, longitudinal measurements. Optical imaging techniques can perform fast, noncontact measurements on a variety of biological samples. However, prior to using these technologies to evaluate tissue function, quantitative relationships between optical and conventional measurement techniques must be established. In this work, we investigate the suitability of label-free fluorescence lifetime imaging (FLIm) as an indirect technique for nondestructively quantifying the changes in mechanical properties of a collagen matrix as a result of cross-link formation.

Collagen is the most abundant protein in the mammalian extracellular matrix[1] and serves a critical role in establishing and maintaining the mechanical properties of various tissues, including bone, skin, blood vessels, and cartilage. Due to its prevalence in mammals and its well-conserved nature, collagen is widely used as a material for tissue engineering applications.[2–4] The capacity to modulate the stiffness of engineered scaffolds is a desirable trait for tissue engineering applications, including instructing differentiation of stem and progenitor cells and producing materials that support the physical requirements of the defect site.[5–7] Moreover, the mechanical properties of a material represent a key element in evaluating the maturation of engineered tissues. Beyond changing the composition, one of the primary methods of controlling the mechanical properties of collagen-based tissue scaffolds is to modify the nature of covalent cross-linking between collagen fibrils.

Glutaraldehyde (GTA) is a widely used chemical cross-linking agent that increases the mechanical properties of a sample.[8–10] However, this enhancement comes at the cost of increased cell toxicity since GTA indiscriminately reacts with amines, amides, and thiol groups on the cells.[9,11–13] GTA cross-linking of collagen is mediated by the reaction of the amine groups of lysine or hydroxylysine residues with the aldehyde groups of GTA.[14] Nonenzymatic collagen cross-links naturally occur in the body under hyperglycemic conditions.[15,16] The formation of advanced glycation end products (AGEs) following the incubation of collagen in a concentrated solution of reducing sugars, such as ribose, induces the formation of nonenzymatic cross-links between lysine and arginine residues on collagen.[17–19]

Cross-links between collagen fibrils are a major source of autofluorescence.[20,21] Multiple studies have measured the intensity, wavelength, and temporal dynamics of fluorescence emission attributed to collagen cross-links.[22–27] Here, we present the first use of a fiber-based imaging system to monitor changes in fluorescence that result from cross-linking treatments. Microscopes and spectrophotometers are extremely powerful

*Address all correspondence to: Benjamin E. Sherlock, E-mail: bsherlock@ucdavis.edu; Laura Marcu, E-mail: lmarcu@ucdavis.edu

1083-3668/2018/$25.00

measurement tools; however, their size and complexity make it challenging to translate these devices into tools that can operate in sterile, space-restricted environments required in the field of tissue engineering. The technique presented here uses a narrow and flexible fiber optic to probe the sample fluorescence, allowing fluorescence lifetime images to be acquired from samples inside a conventional, aseptic biosafety cabinet (BSC). In this work, we investigated the use of FLIm to monitor changes in mechanical properties of collagen hydrogels caused by enhanced cross-link formation. Fluorescence lifetime is a measure of the average time a fluorophore takes to return to its ground state.[28] FLIm is a fiber compatible,[29] inherently ratiometric technique[30] that has a high sensitivity to local changes in a sample's biochemistry.[31] To first order, FLIm is insensitive to factors such as fluorophore density or fluorescence excitation-collection efficiency. These factors can produce artifacts in the images acquired by techniques that rely on fluorescence intensity, especially when imaging in restricted geometries such as inside a tissue bioreactor or as was the case for this work, a BSC.

The goal of this study was to investigate if FLIm could be used as a nondestructive technique to measure changes in collagen hydrogel biochemistry that result from new cross-link formation and to correlate these changes with measurements of hydrogel stiffness. We are specifically and separately targeting two cross-linking agents, GTA and ribose, that are used in the field of regenerative medicine to introduce controlled changes in the mechanical properties of collagen-based biomaterials. We emphasize here that our approach is focused on monitoring the actions of individual cross-linking agents and is not applicable in scenarios where the cross-linking agent is not known *a priori*. Following cross-linking, the fluorescence lifetime of the hydrogels was recorded using our fiber-based multispectral FLIm system. Fluorescence lifetimes are reported from the spectral channels where the signal-to-noise ratio of the recorded fluorescence exceeds 35 dB. Postimaging, the storage modulus or Young's modulus of the hydrogels was measured using rheological or tensile testing, respectively. In the final analysis of the data, a matched sample correlation analysis between changes in fluorescence lifetime and mechanical properties was used to assess the utility of FLIm as a nondestructive tool for monitoring processes of interest to the field of tissue engineering.

2 Methods

2.1 *Collagen Gel Preparation and Cross-link Formation*

Collagen hydrogels derived from rat tail type I collagen were prepared using a commercially available kit (Advanced Biomatrix, San Diego, California). Briefly, nine parts of collagen solution were mixed with one part of neutralization solution on ice and allowed to polymerize for 1 h at 37°C in a humidified incubator (5% CO_2, 21% O_2) to yield hydrogels 8 mm in diameter. The hydrogels used for the GTA and ribose (both from Sigma, St. Louis, Missouri) studies had collagen concentrations of 3.9 and 2.25 mg/mL, respectively.

For the GTA cross-linking studies, hydrogels were incubated in four different concentrations 0.05%, 0.1%, 0.2%, and 1% of GTA for 1 h at room temperature. These concentrations of GTA have been reported to produce significant changes in the viscoelastic properties of collagen hydrogels.[25,32] Control samples were maintained in water under the same conditions. Immediately prior to imaging, hydrogels were washed 2× with water to remove excess GTA. For the ribose cross-linking study, hydrogels were incubated in four different concentrations 62.5, 125, 187.5, and 250 mM of ribose in phosphate-buffered saline (PBS) with 44-mM NaHCO3 (Fisher Scientific, Santa Clara, California) and 25-mM HEPES (Fisher Scientific) buffer for 5 days at 37°C in a humidified incubator (5% CO_2, 21% O_2).[18] Control samples were incubated in PBS with 44-mM $NaHCO_3$ and 25-mM HEPES buffer under the same conditions. Hydrogels were washed 2× with PBS to remove excess sugar prior to imaging. All fluorescence lifetime measurements were conducted with hydrogels immersed in PBS in order to maintain the hydration state and pH of the samples.

2.2 *FLIm Apparatus*

A fiber-coupled FLIm system broadly based on the principal of a previously reported apparatus[33] was used to acquire the lifetime data. A schematic of this system is shown in Fig. 1(a). The light source for fluorescence excitation is a frequency tripled, Nd:YAG microchip laser (STV-02E-1x0, TEEM Photonics, Grenoble, France) that emits 355-nm, 600-ps pulses at a repetition rate of 4 kHz. The average power of the laser incident on the sample surface is 4.51 mW. Fluorescence excitation and emission are guided to and from the sample using a 400-μm core diameter, all silica multimode fiber that has a numerical aperture of 0.22. The lateral extent of the point spread function (PSF) for this fiber was measured using a 13-μm wire phantom coated in fluorescent paint. A fluorescence lifetime image of the phantom was acquired, and the PSF calculated from the mean full width at half maximum of Gaussian fits to 20 adjacent lines in the image that run perpendicular to the wire length. The result of this measurement was a PSF with a lateral width of 251 ± 12 μm. The GTA cross-linked gels were imaged on the benchtop using a 2-m-long fiber, and the ribose-incubated gels were imaged using a 10-m-long fiber, the distal end of which was installed inside a BSC. A wavelength selection module consisting of four dichroic beamsplitters and bandpass filters was used first to separate fluorescence excitation and emission and then to realize four distinct spectral bands for detection. In this work, we report data from the 390 ± 9 nm (CH1), 435 ± 20 nm (CH2), and 510 ± 42 nm (CH3) spectral bands. Each spectral band is coupled to an optical delay line consisting of a 600-μm core diameter multimode fiber (FT600UMT, Thorlabs, Newton, New Jersey). Each delay line has a different length (1, 13, 25, and 37 m for CH1, CH2, CH3, and CH4, respectively), allowing the fluorescence signals in the four spectral bands to be temporally multiplexed on to a single microchannel plate photomultiplier tube (R3809U-50, Hamamatsu, Honshu, Japan) detector. Following amplification by a broadband, low noise amplifier (AM-1607-3000, Miteq, Hauppauge, New York), the temporal dynamics of the fluorescence signals are digitized at a rate of 12.5 GS/s (PXIe-5185, National Instruments, Austin, Texas). Fluorescence lifetimes are extracted from the raw data in postprocessing using a constrained least-squares deconvolution with Laguerre expansion.[34] Exemplar fits and residuals are shown in Figs. 1(d)–1(f). A fluorescence lifetime image is generated by scanning the distal fiber tip over the surface of the sample using a motorized 3-axis translation stage (PROmech LP28, Parker, Cleveland, Ohio). Two 3-axis stages were used in this work, with one being permanently installed inside the BSC to facilitate imaging of the ribose-treated hydrogels, and the other used for benchtop scanning of the GTA cross-linked hydrogels.

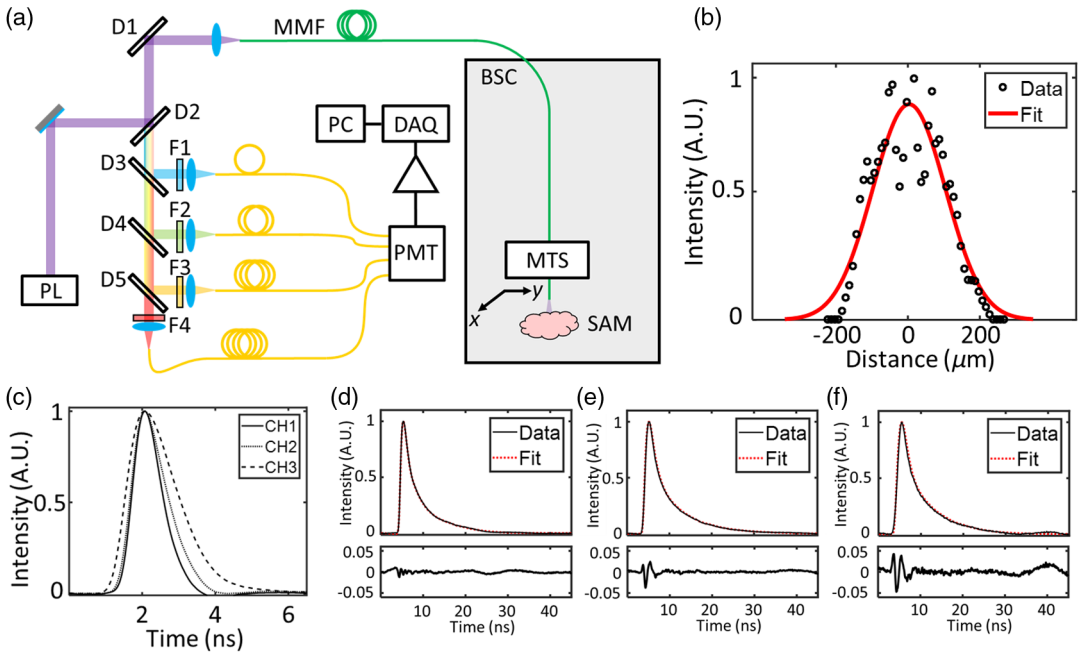

Fig. 1 Fiber-coupled multispectral FLIm system. (a) BSC, biosafety cabinet; D1, 705-nm longpass dichroic mirror; D2, 355-nm longpass dichroic mirror; D3, 405-nm bandpass dichroic mirror; D4: 458-nm bandpass dichroic mirror; D5, 555-nm bandpass dichroic mirror; DAQ, data acquisition board; F1, 390/18-nm bandpass filter; F2, 435/40-nm bandpass filter; F3, 510/84-nm bandpass filter; F4, 607/70-nm bandpass filter; MTS, motorized translation stage; PC, control computer; PL, 355-nm pulsed laser; PMT, photomultiplier tube; and SAM, sample location. (b) Gaussian fit to a measurement of the multimode fiber PSF recorded using a 13-μm wire phantom coated in fluorescent paint. The mean and standard deviation of 20 measurements of the fiber lateral PST were 251 $\pm$ 12 μm (Gaussian full width at half maximum). (c) FLIm system instrument response function recorded in each spectral band used in this work. (d)–(f) Exemplar normalized fluorescence decays, corresponding fits, and residuals in CH1, CH2, and CH3, respectively.

2.3 *Measurement of Mechanical Properties of Collagen Hydrogels*

Rheological measurements were performed using a Discovery HR-2 hybrid stress-controlled rheometer (TA Instruments, New Castle, Delaware) equipped with an 8-mm parallel plate geometry on a stage heated to 37°C as described previously.[35,36] Briefly, hydrogels were tested at a frequency of 0.5 Hz and a logarithmic sweep up to 4% strain 5 points per decade. The shear storage modulus was determined by averaging at least 5 points in the linear viscoelastic region. Tensile testing was conducted using a 5965 Instron machine (Instron, Norwood, Massachusetts) as described previously.[37] Briefly, hydrogels were cut into dog-bone-shaped samples and imaged using a white-light camera. White-light images were processed using ImageJ (National Institutes of Health, Bethesda, Maryland) to extract the sample thickness and width. Samples were then glued at either extremity to two paper strips with a fixed gauge length of 3 mm. A uniaxial strain to failure test was conducted at a strain rate of 1% of the gauge length per second. Force–displacement curves were normalized to specimen dimension data, and the apparent Young's modulus was calculated by least squares fitting the linear portion of the resulting stress–strain curve in MATLAB® (MathWorks, Natick, Massachusetts).

2.4 *Statistics*

For the GTA study, 12 gels were prepared for each of the 5 concentrations of GTA. All gels were imaged using FLIm. Measurements of storage and Young's modulus were made using $n = 6$ gels/group. The uncertainty on the mechanical testing data is reported as the standard deviation of each group. Technical difficulties with the tensile testing apparatus meant that the 1% GTA group could not be reliably measured. A total of four gels ($n = 2$/group) were imaged in the longitudinal GTA study. For the ribose study, due to technical challenges in performing the Young's modulus measurements of the ribose cross-linked gels, only storage moduli ($n = 6$/group) are reported here. In the longitudinal ribose study, $n = 6$ gels were imaged for each of the two groups. The intensity weighted average lifetime[38] and standard deviation of lifetime for individual samples were calculated using the pixel values found inside a circular region of interest centered on the sample and encompassing >75% of the sample area. The fluorescence lifetime attributed to a group in this work was calculated by taking the mean of all individual samples within the group. For all end-point studies, the uncertainty in the fluorescence lifetime of each group was found by taking the standard deviation of the mean lifetimes for each sample. A one-way analysis of variance was used to analyze the significance of differences observed between groups. Significance was defined as $p < 0.05$. A pairwise correlation analysis between changes in fluorescence lifetime and results from rheological (storage modulus) or tensile testing (Young's modulus) was performed using linear regression. To validate the use of linear regression, the Anderson–Darling test was used to test the normality of the fit residuals. For the longitudinal studies, the uncertainty in fluorescence lifetime at each time point is calculated by combining the standard deviation of each sample using standard error propagation.

3 Results

3.1 *GTA Cross-linking Increases Collagen Hydrogel Storage and Young's Modulus and Decreases Mean Fluorescence Lifetime*

Mechanical testing data for collagen hydrogels incubated at room temperature for 1 h in solutions of increasing GTA concentration are presented in Fig. 2. These data show that increasing concentrations of GTA led to increases in hydrogel mechanical properties. Specifically, the storage modulus of the 1% GTA group was 1540 ± 190 Pa, as compared to 240 ± 50 Pa for the control group. Similarly, the Young's modulus of the 0.2% GTA group was measured as 55.5 ± 10.1 kPa, compared with 6.4 ± 1.3 kPa for the control group.

The GTA cross-linked hydrogel mean fluorescence lifetimes recorded in CH1, CH2, and CH3 are presented in Fig. 3. These data show that for increased GTA concentration, and so by inference increased chemical cross-linking of collagen, the mean fluorescence lifetime of each spectral channel decreases. The largest difference was observed in CH2 where the mean lifetime of the 1% GTA group was measured as 2.80 ± 0.06 ns, as

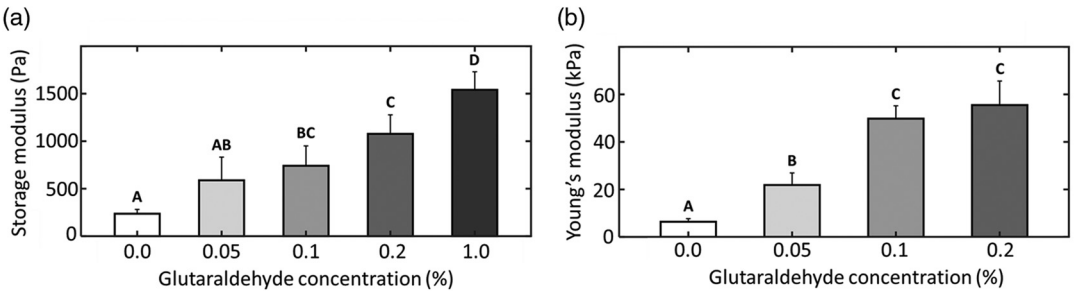

Fig. 2 GTA treatment increases collagen hydrogel storage and Young's modulus. (a) Collagen hydrogel mean storage modulus a function of GTA concentration. (b) Collagen hydrogel mean Young's modulus as a function of GTA concentration. Hydrogels were incubated at room temperature for 1 h prior to measurement. $n = 6$ samples were prepared for each group. Data shown represent samples that underwent successful mechanical testing ($n = 4$ to 6 samples/group). Unique letters label groups that are statistically ($p < 0.05$) different. Error bars are ± 1 standard deviation.

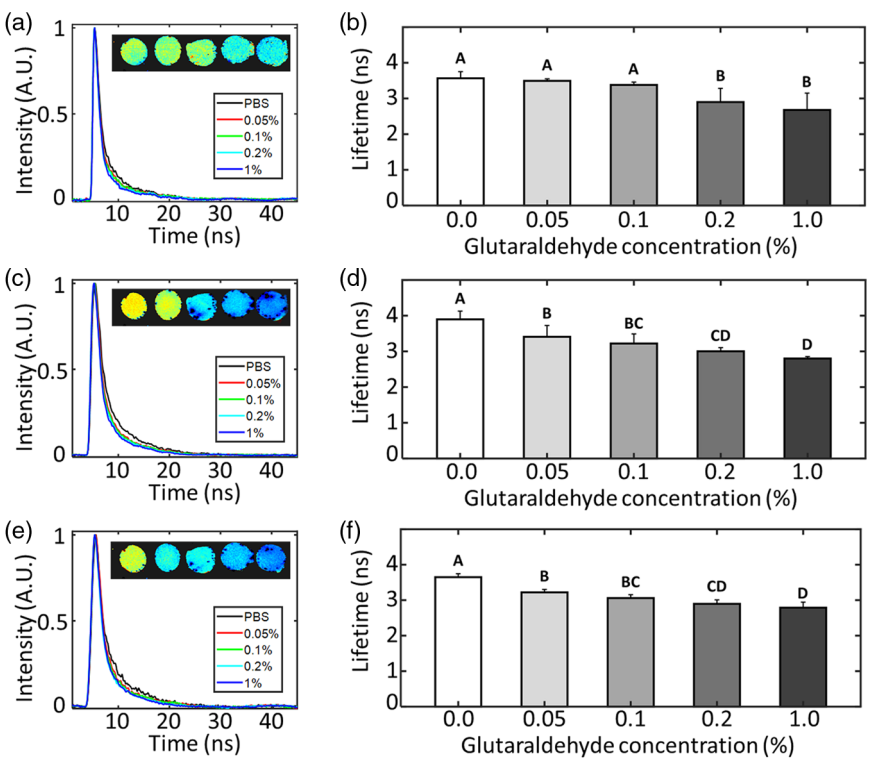

Fig. 3 GTA treatment decreases collagen hydrogel mean fluorescence lifetime. Exemplar raw collagen hydrogel fluorescence decay curves from (a) CH1, (c) CH2, and (e) CH3 spectral bands. Each line shows a decay extracted from a gel incubated in a different concentration of GTA. Insets (left to right): Intensity weighted fluorescence lifetime images of hydrogels incubated in solutions of 0%, 0.05%, 0.1%, 0.2%, and 1% GTA. Color map for these images is scaled from 2 to 5 ns. (b), (d), (f) Collagen hydrogel mean fluorescence lifetime in CH1, CH2, and CH3, respectively, as a function of GTA concentration. Unique letters label groups that are statistically ($p < 0.05$) different. Error bars are ± 1 standard deviation of the means.

compared with 3.90 ± 0.23 ns for the control group. Both trends in the data presented in Figs. 2 and 3 are monotonic with generally statistically significant ($p < 0.05$) differences between groups, suggesting a spectrum of mechanical properties and fluorescent lifetimes that should lend themselves to a correlation analysis.

3.2 *Storage and Young's Moduli of Glutaraldehyde Cross-linked Collagen Hydrogels Present Strong and Specific Correlations with Mean Fluorescence Lifetime*

Figures 4 and 5 show pairwise correlation analyses of mean fluorescence lifetime in three spectral bands plotted as function of storage and Young's modulus, respectively. First degree polynomials fitted to these data reported R^2 values of 0.75, 0.83, and 0.80 for storage modulus and 0.68, 0.72, and 0.74 for Young's modulus for spectral bands CH1, CH2, and CH3, respectively. The Anderson–Darling test indicated that all the fit residuals in Figs. 4 and 5 were normally distributed ($p < 0.05$).

3.3 *FLIm Allows for Longitudinal Monitoring of GTA Cross-linking of Collagen Hydrogels*

The nondestructive nature of FLIm was exploited in a longitudinal measurement of GTA-mediated cross-linking in collagen hydrogels (Fig. 6). Fluorescence lifetime images of two gels immersed in PBS and two gels immersed in 0.2% GTA were recorded at 15-min intervals for the duration of the 1-h cross-linking period. The biggest changes were observed in CH2 where the mean lifetime of the 0.2% GTA group decreased from 3.97 ± 0.37 ns at the beginning to 2.89 ± 0.25 ns at the end of the cross-linking period. By comparison, the control group mean lifetime remained relatively constant, decreasing from a starting value of 3.96 ± 0.37 ns to 3.70 ± 0.47 ns over the 1-h period.

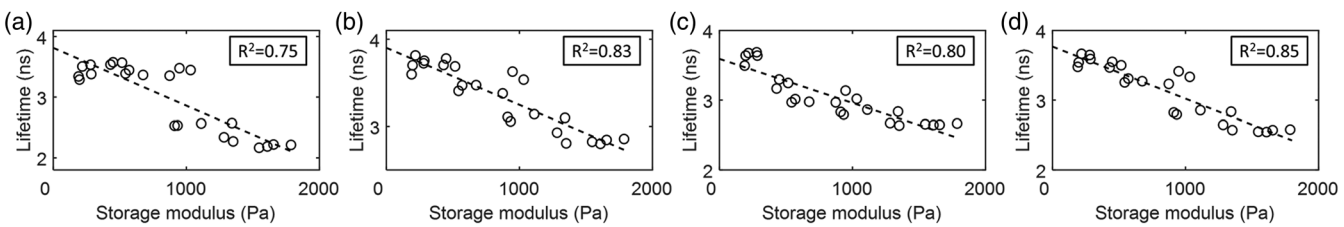

Fig. 4 Mean fluorescence lifetime correlates with storage modulus for GTA-treated collagen hydrogels. Mean fluorescence lifetime recorded in (a) CH1, (b) CH2, and (c) CH3 plotted as a function of storage modulus. (d) Mean of fluorescence lifetimes recorded in all channels plotted as function of storage modulus. In all plots, data are fitted with a first degree polynomial and the corresponding R^2 value reported in the plot legend.

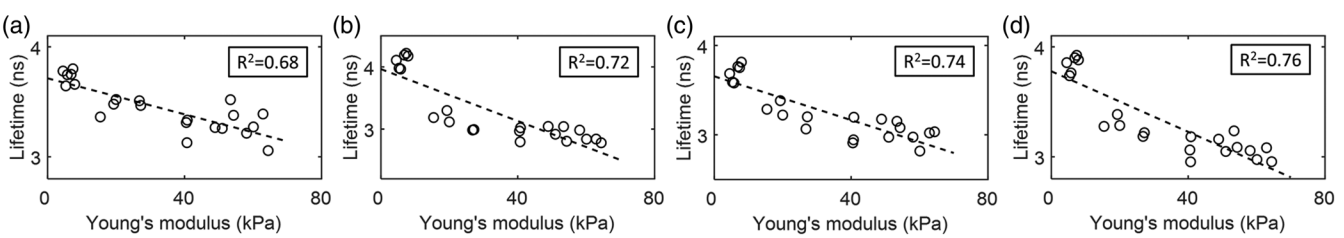

Fig. 5 Mean fluorescence lifetime correlates with Young's modulus for GTA-treated collagen hydrogels. Mean fluorescence lifetime recorded in (a) CH1, (b) CH2, and (c) CH3 plotted as a function of Young's modulus. (d) Mean of fluorescence lifetimes recorded in all channels plotted as function of Young's modulus. In all plots, data are fitted with a first degree polynomial and the corresponding R^2 value reported in the plot legend.

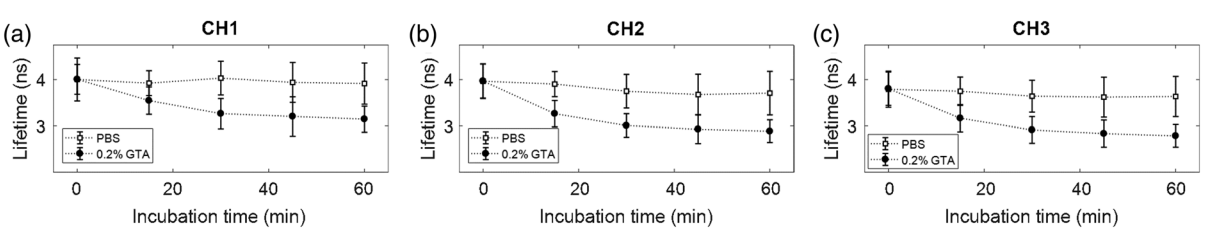

Fig. 6 Fluorescence lifetime can longitudinally monitor the change in autofluorescence of collagen gels treated by 0.2% GTA. Mean fluorescence lifetime recorded in (a) CH1, (b) CH2, and (c) CH3 plotted as a function of collagen hydrogel incubation time in solutions of 0.0% (control) and 0.2% GTA. The measurements were taken from $n = 2$ hydrogels/group that were repeatedly imaged every 15 min for the duration of the 1-h cross-linking period. Error bars are ± 1 standard deviation.

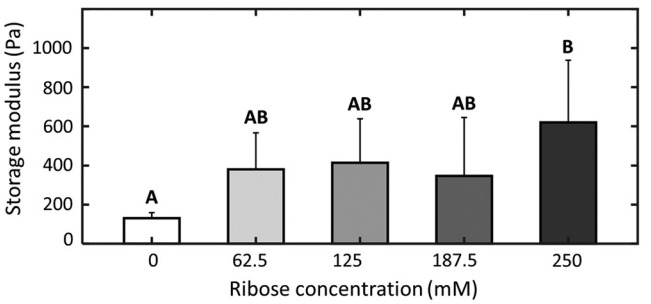

Fig. 7 Ribose treatment increases collagen hydrogel storage modulus. Collagen hydrogel mean storage modulus as a function of ribose solution concentration. Hydrogels were incubated at 37°C in 5% CO_2 for 5 days prior to measurement. $n = 6$ samples were prepared for each group. Data shown represent samples that underwent successful mechanical testing ($n = 4$ to 6 samples/group). Unique letters label groups that are statistically ($p < 0.05$) different. Error bars are ± 1 standard deviation.

3.4 *Ribose Treatment Increases Collagen Storage Modulus and Mean Fluorescence Lifetime*

The storage modulus of 2.25 mg/mL collagen gels incubated in increasing concentrations of ribose solution or PBS for 5 days is presented in Fig. 7. Rheological measurements were only able to detect a statistically significant difference in storage modulus of the highest ribose concentration group (550 ± 320 Pa) over the PBS control group (130 ± 30 Pa). Conversely, as shown in Fig. 8 in each spectral band, FLIm reported large differences between the control and any ribose-treated group, but only small differences between ribose-treated groups. In CH2, the mean fluorescence lifetime of the control group was 4.21 ± 0.07 ns, as compared with 5.63 ± 0.07 ns and 5.70 ± 0.12 ns for the 62.5- and 250-mM ribose groups, respectively. A monotonic increase of mean fluorescence lifetime as a function of ribose concentration is observed in CH1. However, no statistical significant differences were recorded between the 62.5- and 125-mM ribose groups or the 187.5- and 250-mM ribose groups.

3.5 *Storage Modulus of Ribose-Treated Collagen Hydrogels does not Correlate with Mean Fluorescence Lifetime*

Figure 9 shows a pairwise correlation analysis of mean fluorescence lifetime in three spectral bands plotted as function of storage modulus for the ribose-treated collagen gels. The R^2 values for the first degree polynomials do not exceed 0.22 in any of the spectral bands. Furthermore, the Anderson–Darling test

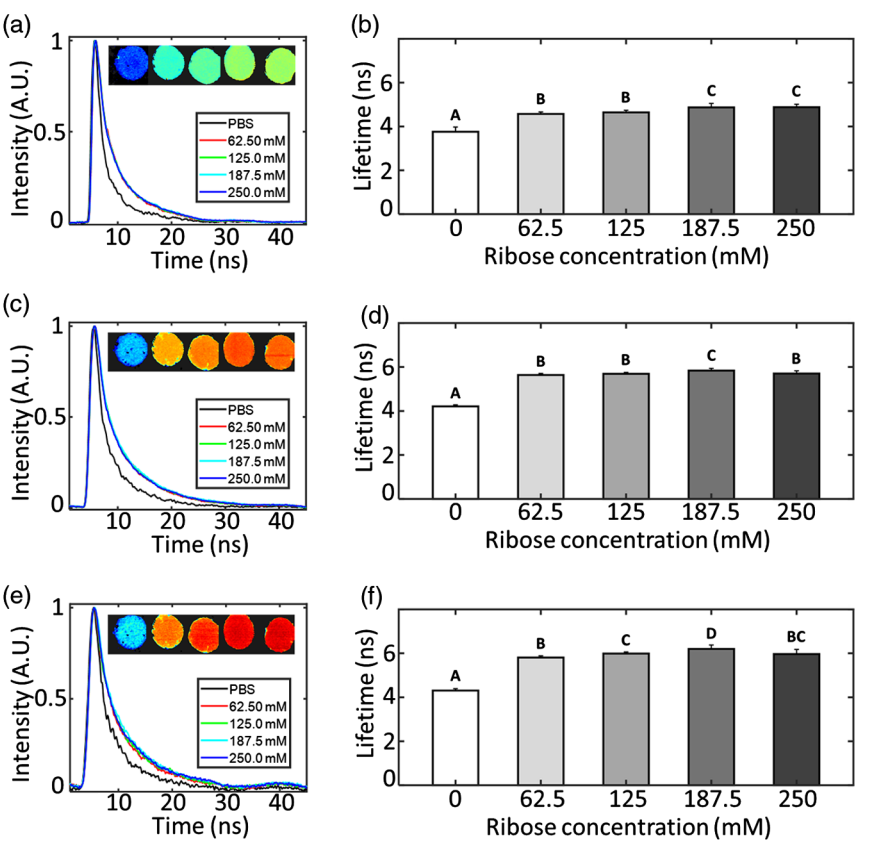

Fig. 8 Ribose treatment increases collagen hydrogel mean fluorescence lifetime. Exemplar raw collagen hydrogel fluorescence decay curves from (a) CH1, (c) CH2, and (e) CH3 spectral bands. Each line shows a decay extracted from a gel incubated in a different concentration of ribose. Insets (left to right): Intensity weighted fluorescence lifetime images of hydrogels cross-linked 0-, 62.5-, 125-, 187.5-, and 250-mM ribose solution. Color map for these images is scaled from 3 to 7 ns. (b), (d), (f) Collagen hydrogel mean fluorescence lifetime in CH1, CH2, and CH3, respectively, as a function of ribose concentration. Unique letters label groups that are statistically ($p < 0.05$) different. Error bars are ± 1 standard deviation of the means.

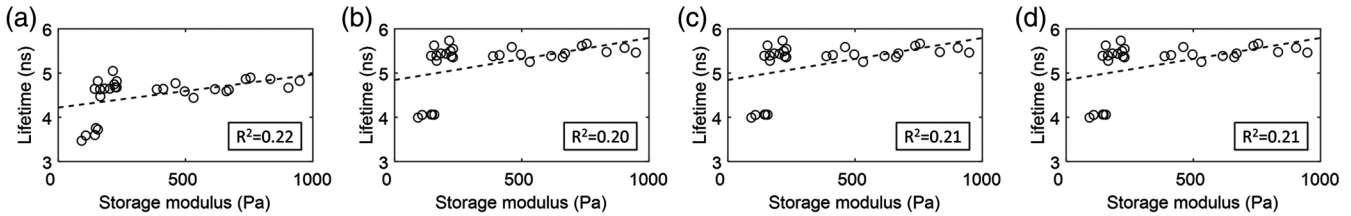

Fig 9 Mean fluorescence lifetime does not correlate with storage modulus for ribose-treated collagen hydrogels. Mean fluorescence lifetime recorded in (a) CH1, (b) CH2, and (c) CH3 plotted as a function of storage modulus. (d) Mean of fluorescence lifetimes recorded in all channels plotted as function of storage modulus. In all plots, data are fitted with a first degree polynomial and corresponding the R^2 value reported in the plot legend.

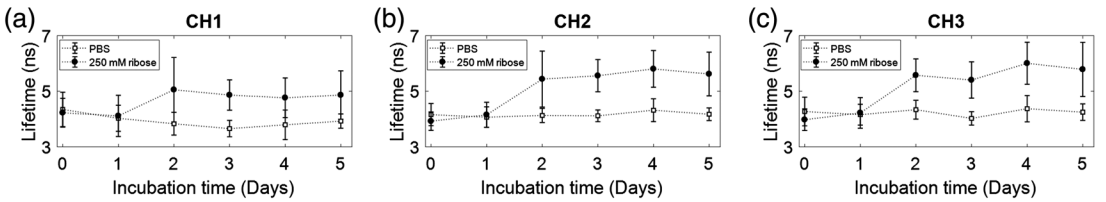

Fig. 10 Fluorescence lifetime can longitudinally monitor changes in collagen hydrogel autofluorescence resulting from ribose incubation. Mean fluorescence lifetime recorded in (a) CH1, (b) CH2, and (c) CH3 plotted as a function of collagen hydrogel incubation time in solutions of 0 (control) and 250-mM ribose solution. The measurements were taken from $n = 6$ hydrogels/group that were repeatedly imaged every day for the duration of the 5-day incubation period. Error bars are ± 1 standard deviation.

indicated that the residuals for all of the fits in Fig. 9 were not normally distributed ($p > 0.05$).

3.6 *FLIm Allows for Longitudinal Monitoring of Ribose-Treated Collagen Hydrogels*

All ribose-treated gels were imaged using a 10-m-long fiber optic, the distal end of which was installed inside a BSC. This was particularly important for the longitudinal monitoring of the ribose treatment where repeated measurements of the same gels in an unsterile environment risked contamination of the ribose solution. Fluorescence lifetime images of the same 6 gels incubated in PBS or 250-mM ribose solution were acquired each day for a 5-day period. The mean fluorescence lifetimes of the two groups in the three spectral channels are shown in Fig. 10. The biggest changes were observed in CH3 where the mean lifetime of the 250-mM ribose group increased from 3.98 ± 0.39 ns at the beginning to 5.79 ± 0.97 ns at the end of the cross-linking period. By comparison, the control group mean lifetime was highly consistent, with initial and final values of 4.24 ± 0.48 ns to 4.25 ± 0.30 ns, respectively, over the 5-day period.

4 Discussion

Fast, nondestructive optical imaging techniques have the potential to lower costs and improve throughput in the field of tissue engineering by replacing slow and destructive conventional testing techniques used for evaluating engineered construct properties. The end-point studies in this work were conducted by acquiring nondestructive FLIm measurements followed by rheological or tensile testing of the same set of collagen hydrogels. Rheology and tensile testing were selected as direct methods to probe changes in the stiffness of the hydrogels. Both methods have been shown to be sensitive to the changes in collagen matrix stiffness caused by enhanced cross-link formation.[18,37,39–41] Since the goal of the study was to correlate functional changes such as mechanical properties to optical parameters, we did not directly measure the formation of collagen cross-links as a result of GTA or ribose treatment.

The different concentrations of GTA produced a set of hydrogels with a spectrum of mechanical properties, with higher GTA concentrations generally producing stiffer hydrogels. A similar distribution of mean fluorescence lifetimes was observed, and the resulting matched sample analysis showed strong correlations between lifetimes and hydrogel storage and Young's moduli. The combination of the strength of the correlations in Fig. 6 and the demonstration in Fig. 7 that changes can be monitored longitudinally without perturbing the cross-linking process suggests that fiber-based FLIm could be used as an effective tool for nondestructive monitoring of changes in sample biomechanics caused by GTA-mediated cross-linking. In the ribose study, the different concentrations of ribose failed to produce a set of samples with a spectrum of mechanical properties as had been reported previously.[18] Instead, statistically significant differences in storage modulus over the control group were only observed for the highest concentration of ribose solution. The storage modulus data did not correlate with mean fluorescence lifetime of the ribose-treated hydrogels. Glycation of collagen catalyzes the production of AGEs, which include a number of fluorescent collagen cross-links, and leads to increased stiffness of the collagen matrix.[42,43] One postulated explanation for the lack of correlation between the mean fluorescence lifetime and storage modulus of ribose-treated collagen hydrogels is that the AGEs responsible for modifying the native collagen fluorescence are not the same or are not formed at the same rate as the AGEs responsible for conveying the new mechanical properties. Several studies in cancellous bone[44] and tendon[45,46] have reported that increasing abundances of pentosidine, a widely studied AGE,[47,48] do not correlate with changes in mechanical properties for those tissues. To test this hypothesis, a detailed biochemical analysis, using

high-performance liquid chromatography or mass spectrometry, would be necessary to uniquely identify which AGEs are formed, when, and how they affect the sample fluorescence and functional properties.

Several pilot human studies have investigated the change in fluorescence lifetime of the eye and skin of type 2 diabetic patients due to increased AGE concentration.[49–51] Each paper reported an increase in the lifetime of fluorescence emitted at wavelengths >420 nm for the diabetic patients compared to healthy patients. Furthermore, recently published results[19] have shown that ribose incubation of decellularized matrices leads to a decrease in fluorescence lifetime at emission wavelengths <390 nm and an increase for wavelengths >390 nm. It is interesting to note that in Ref. 27, the authors report a decrease in fluorescence lifetime as a function of collagen hydrogel glycation time. We postulate that this difference from our study may result from the fluorescence emission being sampled from different spectral regions.

The authors of Refs. 24–26 demonstrated that fluorescence and second-harmonic generation intensity-based techniques could also be used to monitor changes in collagen-based samples resulting from a modification of the sample cross-links. The dynamic range of these intensity-based measurements generally exceeded that of the lifetime-based measurements presented in this work. Collagen and its cross-links are the main extracellular component that resists tension. While both ultrasound elastography[52] and optical coherence tomography[53] have shown utility in nondestructively monitoring gel compressive properties, they have not been used to monitor collagen tensile properties. In this study, we were able to correlate both tensile and compressive properties of collagen gels to FLIm parameters. It is our belief that lifetime remains a promising candidate for nondestructive monitoring of engineered tissue maturation. The inherently ratiometric nature of lifetime measurements makes them well-suited to imaging in nonideal environments such as inside tissue bioreactors or BSCs, where intensity-based techniques may suffer from artifacts.

5 Conclusion

The present study investigated the use of a fiber-based FLIm system to monitor functional changes in collagen hydrogels associated with the application of cross-linking agents GTA and ribose. The nature and extent of collagen cross-linking has a significant impact on tissue stiffness, a key criterion in the generation of engineered tissues. GTA treatment at different concentrations produced collagen hydrogels with a spectrum of mechanical properties and mean fluorescence lifetimes, which revealed strong correlations when plotted against one another. A longitudinal experiment involving the repeated imaging of four hydrogels showed that FLIm could be used to nondestructively probe the progression of the GTA cross-linking process. Both findings suggest significant promise for fiber-based FLIm as a fast and effective tool to nondestructively infer the mechanical properties of collagen-based materials undergoing GTA cross-linking. Ribose treatment failed to produce a measurable spectrum of collagen hydrogel mechanical properties or mean fluorescence lifetimes. Furthermore, the two datasets showed no clear evidence of correlation, suggesting that additional studies need to be performed before a conclusive statement about the utility of fluorescence lifetime for monitoring ribose mediated nonenzymatic cross-linking can be made. All ribose-treated hydrogels were imaged using a 10-m-long optical fiber, the distal end of which was installed inside a BSC, indicating that fiber-based FLIm can be deployed in environments where taking measurements using conventional microscopes is highly challenging. In summary, we have demonstrated that FLIm can provide a nondestructive approach to monitoring changes in functional properties of samples undergoing specific, controlled biochemical treatments that are known *a priori*. We believe these findings have significant implications for the field of regenerative medicine. Nondestructive analysis of tissue properties has the potential to increase sample throughput by avoiding destruction of engineered tissues during measurement, monitor sample maturation over time, and serve as a quality control for engineered samples at various stages of their development.

Disclosures

The authors confirm that there are no known conflicts of interest associated with this publication and there has been no significant financial support for this work that could have influenced its outcome.

Acknowledgments

This research was made possible by a grant from the California Institute for Regenerative Medicine (Grant No. RT3-07981) to J.K.L. and L.M. A.H., J.C., and K.A. would like to acknowledge financial support from the National Institutes of Health Grant No. R01AR067821. J.N.H. is grateful for financial support from the National Defense Science and Engineering Graduate Fellowship (No. 32 CFR 168a) and the ARCS Foundation. D.M. is grateful for financial support through the California Institute for Regenerative Medicine UC Davis Stem Cell Training Program (No. CIRM TG2-01163) and an industry/campus supported fellowship under the Training Program in Biomolecular Technology (No. T32-GM008799) at the University of California, Davis. The contents of this publication are solely the responsibility of the authors and do not necessarily represent the official views of CIRM or any other agency of the State of California.

References

1. D. Baltimore, *Molecular Cell Biology*, W. H. Freeman, New York (2000).
2. J. H. Choi et al., "Adipose tissue engineering for soft tissue regeneration," *Tissue Eng. Part B. Rev.* **16**(4), 413–426 (2010).
3. R. Parenteau-Bareil, R. Gauvin, and F. Berthod, "Collagen-based biomaterials for tissue engineering applications," *Materials* **3**(3), 1863–1887 (2010).
4. M. G. Haugh et al., "Crosslinking and mechanical properties significantly influence cell attachment, proliferation, and migration within collagen glycosaminoglycan scaffolds," *Tissue Eng. Part A* **17**(9–10), 1201–1208 (2011).
5. J. L. Drury and D. J. Mooney, "Hydrogels for tissue engineering: scaffold design variables and applications," *Biomaterials* **24**(24), 4337–4351 (2003).
6. J. J. Pancrazio, F. Wang, and C. A. Kelley, "Enabling tools for tissue engineering," *Biosens. Bioelectron.* **22**(12), 2803–2811 (2007).
7. H. Nitzsche et al., "Fabrication and characterization of a biomimetic composite scaffold for bone defect repair," *J. Biomed. Mater. Res.–Part A* **94**(1), 298–307 (2010).
8. M. D. Harriger et al., "Glutaraldehyde crosslinking of collagen substrates inhibits degradation in skin substitutes grafted to athymic mice," *J. Biomed. Mater. Res.* **35**(2), 137–145 (1997).
9. V. Perez-Puyana, A. Romero, and A. Guerrero, "Influence of collagen concentration and glutaraldehyde on collagen-based scaffold properties," *J. Biomed. Mater. Res.–Part A* **104**(6), 1462–1468 (2016).

10. T. P. Sarac et al., "In vivo and mechanical properties of peritoneum/fascia as a novel arterial substitute," *J. Vasc. Surg.* **41**(3), 490–497 (2005).
11. J. E. Gough, C. A. Scotchford, and S. Downes, "Cytotoxicity of glutaraldehyde crosslinked collagen/poly(vinyl alcohol) films is by the mechanism of apoptosis," *J. Biomed. Mater. Res.* **61**(1), 121–130 (2002).
12. V. Charulatha and A. Rajaram, "Influence of different crosslinking treatments on the physical properties of collagen membranes," *Biomaterials* **24**(5), 759–767 (2003).
13. Z. Tian, W. Liu, and G. Li, "The microstructure and stability of collagen hydrogel cross-linked by glutaraldehyde," *Polym. Degrad. Stab.* **130**, 264–270 (2016).
14. L. H. H. Olde Damink et al., "Glutaraldehyde as a crosslinking agent for collagen-based biomaterials," *J. Mater. Sci. Mater. Med.* **6**(8), 460–472 (1995).
15. A. Goldin et al., "Advanced glycation end products: sparking the development of diabetic vascular injury," *Circulation* **114**(6), 597–605 (2006).
16. J. G. Snedeker and A. Gautieri, "The role of collagen crosslinks in ageing and diabetes—the good, the bad, and the ugly," *Muscles Ligaments Tendons J.* **4**(3), 303–308 (2014).
17. M.-A. Mycek and B. W. Pogue, *Handbook of Biomedical Fluorescence*, CRC Press, Boca Raton, Florida (2003).
18. R. Roy, A. Boskey, and L. J. Bonassar, "Processing of type I collagen gels using nonenzymatic glycation," *J. Biomed. Mater. Res. Part A* **93**(3), 843–851 (2009).
19. D. Mitra et al., "Detection of pentosidine cross-links in cell-secreted decellularized matrices using time resolved fluorescence spectroscopy," *ACS Biomater. Sci. Eng.* **3**(9), 1944–1954 (2017).
20. N. Kollias et al., "Endogenous skin flourescence includes bands that may serve as quantitative markers of aging and photoaging," *J. Invest. Dermatol.* **111**(5), 776–780 (1998).
21. L. Marcu, P. M. W. French, and D. S. Elson, *Fluorescence Lifetime Spectroscopy and Imaging: Principles and Applications in Biomedical Diagnostics*, CRC Press, Boca Raton, Florida (2014).
22. E. Fujimori, "Cross-linking and fluorescence changes of collagen by glycation and oxidation," *Biochim. Biophys. Acta (BBA)-Protein Struct. Mol. Enzymol.* **998**(2), 105–110 (1989).
23. J. J. Tomasek et al., "Diabetic and age-related enhancement of collagen-linked fluorescence in cortical bones of rats," *Life Sci.* **55**(11), 855–861 (1994).
24. H. G. Sundararaghavan et al., "Genipin-induced changes in collagen gels: correlation of mechanical properties to fluorescence," *J. Biomed. Mater. Res.–Part A* **87**(2), 308–320 (2008).
25. C. B. Raub et al., "Noninvasive assessment of collagen gel microstructure and mechanics using multiphoton microscopy," *Biophys. J.* **92**(6), 2212–2222 (2007).
26. V. Lutz et al., "Impact of collagen crosslinking on the second harmonic generation signal and the fluorescence lifetime of collagen autofluorescence," *Skin Res. Technol.* **18**(2), 168–179 (2012).
27. S. Fukushima et al., "Decrease in fluorescence lifetime by glycation of collagen and its application in determining advanced glycation end-products in human dentin," *Biomed. Opt. Express* **6**(5), 1844 (2015).
28. X. F. Wang, T. Uchida, and S. Minami, "A fluorescence lifetime distribution measurement system based on phase-resolved detection using an image dissector tube," *Appl. Spectrosc.* **43**(5), 840–845 (1989).
29. H. Xie et al., "Multispectral scanning time-resolved fluorescence spectroscopy (TRFS) technique for intravascular diagnosis," *Biomed. Opt. Express* **3**(7), 1521–1533 (2012).
30. J. McGinty et al., "In vivo fluorescence lifetime optical projection tomography," *Biomed Opt Express* **2**(5), 1340–1350 (2011).
31. J. R. Lakowicz et al., "Fluorescence lifetime imaging," *Anal. Biochem.* **202**(2), 316–330 (1992).
32. M. T. Sheu et al., "Characterization of collagen gel solutions and collagen matrices for cell culture," *Biomaterials* **22**(13), 1713–1719 (2001).
33. D. R. Yankelevich et al., "Design and evaluation of a device for fast multispectral time-resolved fluorescence spectroscopy and imaging," *Rev. Sci. Instrum.* **85**(3), 034303 (2014).
34. J. Liu et al., "A novel method for fast and robust estimation of fluorescence decay dynamics using constrained least-squares deconvolution with Laguerre expansion," *Phys. Med. Biol.* **57**(4), 843–865 (2012).
35. K. C. Murphy et al., "Hydrogel biophysical properties instruct coculture-mediated osteogenic potential," *FASEB J.* **30**(1), 477–486 (2016).
36. S. S. Ho et al., "Increased survival and function of mesenchymal stem cell spheroids entrapped in instructive alginate hydrogels," *Stem Cells Transl. Med.* **5**(6), 773–781 (2016).
37. E. A. Makris, J. C. Hu, and K. A. Athanasiou, "Hypoxia-induced collagen crosslinking as a mechanism for enhancing mechanical properties of engineered articular cartilage," *Osteoarthritis Cartilage* **21**(4), 634–641 (2013).
38. A. Sillen and Y. Engelborghs, "The correct use of 'average' fluorescence parameters," *Photochem. Photobiol.* **67**(5), 475–486 (1998).
39. W. M. Elbjeirami et al., "Enhancing mechanical properties of tissue-engineered constructs via lysyl oxidase crosslinking activity," *J. Biomed. Mater. Res. Part A* **66A**(3), 513–521 (2003).
40. M. L. Wong et al., "The role of protein solubilization in antigen removal from xenogeneic tissue for heart valve tissue engineering," *Biomaterials* **32**(32), 8129–8138 (2011).
41. T. Schuetz et al., "The microstructure of collagen type I gel cross-linked with gold nanoparticles," *Colloids Surfaces B Biointerfaces* **101**(1), 118–125 (2013).
42. N. Verzijl et al., "Crosslinking by advanced glycation end products increases the stiffness of the collagen network in human articular cartilage," *Arthritis Rheumatol.* **46**(1), 114–123 (2002).
43. L. Séro et al., "Tuning a 96-well microtiter plate fluorescence-based assay to identify AGE inhibitors in crude plant extracts," *Molecules* **18**(11), 14320–14339 (2013).
44. N. M. B. K. Willems et al., "Higher number of pentosidine cross-links induced by ribose does not alter tissue stiffness of cancellous bone," *Mater. Sci. Eng. C* **42**, 15–21 (2014).
45. T. T. Andreassen, H. Oxlund, and C. C. Danielsen, "The influence of non-enzymatic glycosylation and formation of fluorescent reaction products on the mechanical properties of rat tail tendons," *Connect. Tissue Res* **17**(1), 1–9 (1988).
46. J. E. Marturano et al., "Characterization of mechanical and biochemical properties of developing embryonic tendon," *Proc. Natl. Acad. Sci. U. S. A.* **110**(16), 6370–6375 (2013).
47. R. Sanguineti et al., "Pentosidine effects on human osteoblasts in vitro," *Ann. N. Y. Acad. Sci.* **1126**, 166–172 (2008).
48. L. Karim et al., "Differences in non-enzymatic glycation and collagen cross-links between human cortical and cancellous bone," *Osteoporosis Int.* **24**(9), 2441–2447 (2013).
49. D. Schweitzer et al., "Fluorescence lifetime imaging ophthalmoscopy in type 2 diabetic patients who have no signs of diabetic retinopathy," *J. Biomed. Opt.* **20**(6), 061106 (2015).
50. J. Schmidt et al., "Fundus autofluorescence lifetimes are increased in non-proliferative diabetic retinopathy," *Acta Ophthalmol.* **95**(1), 33–40 (2017).
51. J. Blackwell et al., "In vivo time-resolved autofluorescence measurements to test for glycation of human skin," *J. Biomed. Opt.* **13**(1), 014004 (2008).
52. X. Hong, J. P. Stegemann, and C. X. Deng, "Microscale characterization of the viscoelastic properties of hydrogel biomaterials using dual-mode ultrasound elastography," *Biomaterials* **88**, 12–24 (2016).
53. H.-J. Ko et al., "Optical coherence elastography of engineered and developing tissue," *Tissue Eng.* **12**(1), 63–73 (2006).

Benjamin E. Sherlock is a project scientist at the University of California, Davis. He received his MSci degree in physics from the University of Durham, UK, in 2006, and his DPhil in atomic and laser physics from the University of Oxford, UK, in 2012. His research interests include innovative biomedical imaging systems, nonlinear microscopy, fiber-based multimodal imaging, and fundamental light–matter interactions. He is a member of SPIE.

Biographies for the other authors are not available.